Arteriolar network architecture and vasomotor function with ageing in mouse gluteus maximus muscle

Shawn E. Bearden[1], Geoffrey W. Payne[1], Alia Chisty[2] and Steven S. Segal[1,2]

The John B. Pierce Laboratory and [1]Departments of Cellular & Molecular Physiology and [2]Department of Molecular, Cellular and Developmental Biology, Yale University, New Haven, CT 06519, USA

Physical diminishes with ageing, but little is known of how the microvascular supply to skeletal muscle fibres is affected. To test the hypothesis that ageing alters blood flow control, we investigated network architecture and vasomotor responses of arterioles in the gluteus maximus muscle of young (2–3 months), adult (12–14 months) and old (18–20 months) C57BL6 male mice ($n = 83$) (Young, Adult and Old, respectively). Microvascular casts revealed that the total number, length and surface area of arteriolar segments (diameter, 10–50 μm) were not significantly different across age-groups. However, for arterioles with diameter of 30 μm, tortuosity and branch angles increased with age ($P < 0.05$). In anaesthetized mice, second-order (2A) distributing arterioles had similar resting (17 ± 1 μm) and maximal (37 ± 1 μm) diameters and similar responsiveness to cumulative (10^{-10}—10^{-4} M) superfusion of acetylcholine or phenylephrine. With superfusate oxygen level raised from 0 to 21%, 2A arteriolar constriction in Young (11 ± 1 μm) was greater ($P < 0.05$) than Adult and Old (5 ± 1 μm). Observed 1 mm upstream from microiontophoresis of ACh (1 μA, 1 s), conducted vasodilatation was 10 ± 1 μm in Young, 17 ± 1 μm in Adult and 6 ± 1 μm in Old ($P < 0.05$). With muscle contractions (2, 4 and 8 Hz; 30 s) arteriolar diameter increased similarly across age-groups (6 ± 1, 11 ± 1 and 18 ± 1 μm, respectively). Muscle mass and active tension were similar across age-groups yet postcontraction vasodilatation recovered more rapidly in Old *versus* Adult and Young ($P < 0.05$). With arteriolar network architecture maintained during ageing, the impairment in conducted vasodilatation and attenuation of postcontraction vasodilatation may compromise exercise tolerance.

(Received 17 May 2004; accepted after revision 14 September 2004; first published online 16 September 2004)
Corresponding author S. S. Segal: The John B. Pierce Laboratory, Yale University School of Medicine, 290 Congress Ave, New Haven, CT 06519, USA. Email: sssegal@jbpierce.org

Physical activity reflects a dynamic interplay between skeletal muscle and its vascular supply. The tolerance for exercise decreases with advancing age, which can promote a sedentary lifestyle and increase the risk of injury and disease (Dutta *et al.* 1997). In humans, a decline in physical performance with ageing has been associated with sarcopenia, reflecting muscle fibre atrophy as well as the loss of motor units (Lexell, 1995). Ageing can also reduce the ability to increase blood flow to active skeletal muscle, as shown in rats (Irion *et al.* 1987) and humans (Wahren *et al.* 1974; Proctor *et al.* 1998; Lawrenson *et al.* 2003). In light of the dependence of physical performance on muscle blood flow, it is remarkable that little is known of how ageing affects the microvascular networks that supply skeletal muscle fibres.

A key determinant of the ability to perform aerobic exercise is a robust arteriolar network to deliver and control blood flow. Indeed, the number, dimensions and branching characteristics of individual arteriolar segments collectively determine the conductance of the intramuscular resistance network. In the cremaster muscle of Fischer-344 rats, arteriolar diameters and segment lengths tended to increase from 12 to 24 months of age (Cook *et al.* 1992). Conversely, in the ear of the mouse, arteriolar network architecture remained stable through 20 months of age (Vollmar *et al.* 2000). However, it is unknown whether (and if so, how) changes occur with ageing in the architecture of skeletal muscles that are involved in locomotion.

The matching of blood flow to metabolic demand of active muscle fibres involves the integration of vasodilator responses within arteriolar networks (Segal, 1991; Cohen & Sarelius, 2002). This coordinated activity

S. E. Bearden and G. W. Payne contributed equally to this work

DOI: 10.1113/jphysiol.2004.068262

is achieved through cell-to-cell conduction along the arteriolar wall (Segal & Duling, 1989; Hungerford *et al.* 2000; Figueroa *et al.* 2003). However, the effect of ageing on the ability to coordinate vasodilator responses along arterioles is unknown. As inferred from studies of arterioles isolated from hindlimb skeletal muscles of old (24 months) Fischer-344 rats (Muller-Delp *et al.* 2002*a*,*b*), changes in vasomotor responses can alter blood flow control *in vivo*. Nevertheless, there is a paucity of information concerning whether (and if so, how) ageing may affect the functional properties of arterioles controlling blood flow to active muscle fibres. In addition to vasodilatation during activity, the restoration of muscle function may be enhanced by the ability to sustain vasodilatation into the recovery period by promoting metabolite removal and replenishing energy stores.

In the present study, we tested the hypothesis that ageing of skeletal muscle leads to adaptations in: (1) the architecture of arteriolar networks; (2) the reactivity of arteriolar smooth muscle and endothelial cells; (3) the ability of arterioles to conduct vasodilatation; and (4) arteriolar responses to skeletal muscle contraction. To investigate these relationships in a locomotor muscle of the mouse, we developed the gluteus maximus muscle as a model system. From microvascular casts, three-dimensional maps of complete arteriolar networks arising from the inferior gluteal artery were evaluated for changes in architecture and topology. Using intravital microscopy, responses of second-order (2A) arterioles to agonists and to muscle contraction were evaluated because these branches serve as the key distributing vessels in the mouse gluteus maximus muscle.

Methods

Animal care

Procedures were approved by the Animal Care and Use Committee of The John B. Pierce Laboratory and performed in accord with the National Institutes of Health (NIH) *Guide for the Care and Use of Laboratory Animals*. Experiments were performed on male C57BL6 mice (25–35 g, $n = 83$, Jackson Laboratories, Bar Harbour, ME, USA and Harlan, Indianapolis, IN, USA). Mice from three age-groups were studied: Young (2–3 months); Adult (12–14 months); and Old (18–20 months). Mice were housed at 24°C on a 12 h light−12 h dark cycle with fresh food and water *ad libitum*. Body mass was measured before each experiment.

Experiment 1: arteriolar network architecture

Vascular casting. Mice were deeply anaesthetized with pentobarbital sodium (60 mg kg^{-1}, intraperitoneal injection) and perfused with fixative (phosphate buffered saline (PBS) containing 10 U ml^{-1} heparin and 10^{-5} M sodium nitroprusside, at pH 7.4, followed by 3% paraformaldehyde dissolved in PBS) through a cannula inserted in the ascending aorta with effluent from an opening made in the right atrium. Using the same cannula, the vasculature was then filled with a white silicone-based compound (Microfil; Flowtech Inc., Carver, MA, USA), which was allowed to harden overnight. The right gluteus maximus muscle was then excised and cleared (3 h in each of 30%, 60% and 90% glycerin in PBS and stored in 100% glycerin), which makes the tissue translucent and the opaque vascular cast more distinct. Casts were analysed within 1–2 weeks and are stable in this condition for several months.

Arteriolar network analyses. Whole-mount muscle preparations were placed on the stage of a Nikon E600 microscope instrumented for creating digitized three-dimensional maps using a Neurolucida system (MicroBrightfield, Williston, VT, USA). In each muscle ($n = 5$ per age-group), the entire arteriolar network arising from the inferior gluteal artery (maximum diameter, 52–57 μm) was mapped through its terminal branches. Images were acquired through Nikon Plan Fluor 10X and 20X objectives (NA, 0.30 and 0.50, respectively) coupled to a cooled CCD camera (Microfire, Optronics, Goleta, CA, USA) and displayed on a computer monitor (final magnification, 380X and 760X, respectively). Three-dimensional mapping was performed using an integrated joystick control of the microscope stage by stepper motors (Ludl Electronic, Hawthorne, NY, USA). Each muscle was scanned while 'tracing' the network throughout the muscle with diameter information controlled by adjusting the size of the tracing icon. In this manner, complete networks were converted into X–Y–Z coordinates with spatial resolution $< 2\,\mu$m. Using the same tracing procedures, muscle perimeters were outlined to calculate muscle surface area which, along with muscle mass, was used to determine whether muscles atrophied with ageing.

In conjunction with MicroBrightfield, software was developed to perform computerized analyses of digitized microvascular networks. Complete arteriolar networks were analysed for: number of segments, branch angles, tortuosity, segment lengths and segment surface areas. A 'segment' was defined as the portion of an arteriole lying between consecutive branches. Data were organized according to segment diameter in bins of 11–20, 21–30, 31–40 and 41–50 μm. Segment length was defined as the distance between successive branch points. Branch angle was defined as the angle between daughter branches at each bifurcation and was categorized according to the diameter of the smaller daughter segment. Tortuosity was defined as the ratio of segment length to the straight-line distance between segment end-points. Luminal surface areas were calculated assuming that the arterioles were

cylindrical. For each muscle, a mean value for each of these measures was calculated for each 10-μm diameter bin. The total segment length in each diameter bin was calculated for each muscle as the sum of all respective individual segment lengths. The total surface area in each diameter bin was calculated for each muscle as the sum of all respective individual segment surface areas. Thus, with five mice studied for arteriolar network architecture in each age-group, $n = 5$ for each variable in the analysis and presentation of these data.

Wet and dry muscle mass. In three additional mice per age-group, gluteus maximus muscles were excised bilaterally and weighed for wet muscle mass. These muscles were then dried at 50°C for 4 h and re-weighed for dry muscle mass.

Experiment 2: arteriolar reactivity and conducted vasodilatation

Muscle preparation and intravital microscopy. Mice were anaesthetized with pentobarbital sodium (25 mg ml^{-1}; 50 mg kg^{-1}, intraperitoneal injection), which was supplemented as needed to prevent withdrawal from toe pinch. The mouse was placed prone on an acrylic platform. Oesophageal temperature was maintained at 37–38°C using radiant heat. With the aid of a stereomicroscope, skin overlying the left gluteus maximus muscle was removed. The proximal edge of the muscle was freed from its origin along the spine and reflected away from the mouse while preserving its neurovascular supply and insertion onto the femur. The muscle was spread evenly to approximate *in situ* dimensions and the proximal edge pinned onto a transparent pedestal (Sylgard 184; Dow Corning, Midland, MI, USA) while being superfused with bicarbonate-buffered physiological salt solution (PSS; 34°C, pH 7.4) of the following composition (mM): NaCl 137, KCl 4.7, $MgSO_4$ 1.2, $CaCl_2$ 2 and $NaHCO_3$ 18. The PSS was equilibrated with 5% CO_2–95% N_2 except where noted. All chemicals and reagents were purchased from Sigma-Aldrich Co. (St Louis, MO, USA) or J. T. Baker (Phillipsburg, NJ, USA).

The completed preparation was transferred to the stage of an intravital microscope (modified model 20T; Zeiss) and allowed to equilibrate for at least 30 min. Using brightfield illumination (ACH/APL condenser; NA, 0.32), arterioles were observed through a Zeiss UD40 objective (NA, 0.41) coupled to a video camera (C2400; Hamamatsu, Japan); final magnification on the video monitor (model PVM-132; Sony, Japan) was 950X. Internal vessel diameter was determined as the distance between luminal edges using a video caliper (modified model 321; Colorado Video Inc, Boulder, CO, USA) with spatial resolution ≤ 1 μm. Data were acquired at 40 Hz using PowerLab (model 8S; AD Instruments, Castle Hill, Australia) coupled to a laboratory computer.

Second-order (2A) branches of the arteriolar network were chosen for study because they are ideally positioned to control the distribution of blood flow within the muscle (Fig. 1). Due to the consistent overall architecture of the network among animals (see Results), these data were obtained from approximately the same region of each preparation (Fig. 1). Diameter was measured at rest under control conditions and after elevating the superfusate oxygen level to 21% (with 5% CO_2, balance N_2) for 10 min. At the end of each experiment, maximum diameter was recorded following topical application of 10^{-5} M sodium nitroprusside (SNP) and the mouse was given an overdose of sodium pentobarbital (intraperitoneal injection).

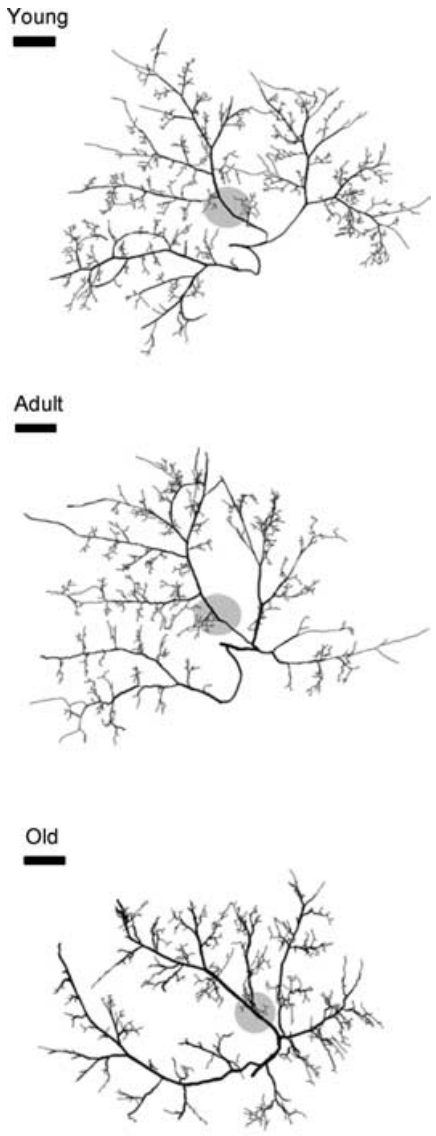

Figure 1. Images of 3-dimensional maps of the arteriolar network arising from the inferior gluteal artery in the mouse gluteus maximus muscle
The overall arteriolar network topology was conserved with ageing. Shaded discs indicate the region where data were obtained in Experiments 2 and 3. Scale bars indicate 1 mm.

Arteriolar reactivity. The effects of acetylcholine (ACh; endothelium-dependent vasodilator) and phenylephrine (PE; α_1-selective smooth muscle-dependent vasoconstrictor) were evaluated by cumulative addition (10^{-10}–10^{-4} M) to the superfusion solution. In half of these experiments, responses to ACh were evaluated, resting diameter was allowed to recover, and responses to PE were then evaluated. In the remaining experiments, responses to PE were evaluated before those to ACh. At each agonist concentration, arteriolar diameter was allowed to stabilize for at least 2 min and recorded before the next increment. Working concentrations were prepared fresh daily and administered after diluting at least 100-fold in fresh PSS. Following ACh or PE exposure, resting diameter typically recovered within 30 min of restoring control superfusate.

Conducted vasodilatation. Micropipettes with internal tip diameters of 1–2 μm were pulled (P-97; Sutter Instruments, Novato, CA, USA) from borosilicate glass capillary tubes (GC120F-10; Warner Instruments, Hamden, CT, USA) and backfilled with 1 M ACh dissolved in deionized H_2O. A micropipette was secured in a holder containing a Ag–AgCl wire and positioned with its tip adjacent to a 2A arteriole using a micromanipulator mounted to the acrylic platform. This configuration allowed movement of the entire preparation without disturbing the position of the micropipette relative to the arteriole. ACh was delivered as 1 μA pulses of 250, 500, 750 and 1000 ms duration using microiontophoresis (model 260; World Precision Instruments, Sarasota, FL, USA); a constant retaining current (200 nA) prevented leak of ACh from the micropipette tip. A Ag–AgCl wire mounted at the edge of the preparation served as the reference electrode.

Experiment 3: arteriolar responses and active tension with muscle contraction

Contraction-induced and recovery of vasodilatation. The gluteus maximus muscle was prepared for intravital microscopy as described for Experiment 2. Electrodes were prepared from 90% Pt−10% Ir wire (diameter, 250 μm) and positioned on either side of the muscle for field stimulation. Muscle contraction was driven with monophasic square-wave pulses (0.1 ms) delivered through an SIU5 stimulus isolation unit driven by an S48 stimulator (Grass, Quincy, MA, USA). The muscle was stimulated at 2, 4 and 8 Hz for 30 s at 100 V. For all experiments, arteriolar diameter was recorded prior to the onset of contraction and from the end of contraction throughout recovery. Although diameter measurements were typically not obtained during the period of contraction (due to tissue displacement), it was confirmed in several experiments that arterioles consistently dilated to a stable value during contractions. The recovery of arteriolar tone following each contraction was characterized by determining the time required to return to within 37% (1/e) of the original baseline diameter.

Active tension production. The gluteus maximus ($n = 4$ mice per age-group) was prepared as above except that muscles were clamped instead of pinned along their proximal edge. The clamp was attached to a load beam (LCL-1136; Omega, Stamford, CT, USA; resolution, $\pm$ 0.1 g) coupled to a Transbridge amplifier (TBM-4; World Precision Instruments, Sarasota, FL, USA). The load beam was held by a micrometer in line with the orientation of muscle fibres. Optimal muscle length (L_o) for twitch tension was established and followed by a single contraction (300 ms, 200 Hz, 100 V) to measure maximal tetanic contraction (P_o). Muscles were then stimulated at 2, 4 and 8 Hz as above to measure peak active tension during respective contractions. To define frequency–force characteristics, muscles were stimulated (300 ms, 100 V) at 5, 10 and 20–200 Hz (in 20 Hz increments) and these data were normalized to P_o for presentation. To calculate specific tension production (mN (mm cross-sectional area)$^{-2}$), muscle fibre length ($\pm$ 0.1 mm) and wet weight ($\pm$ 0.1 mg) were measured at the end of each experiment. Muscle density was assumed to be 1.056 mg mm^{-3}.

Verification of muscle recruitment during locomotion. To confirm that the mouse gluteus maximus muscle is recruited during locomotion, two protocols were performed in Young. In the first protocol, muscle glycogen content (kit 439–90901; Wako USA, Richmond, VA, USA) was measured bilaterally in whole gluteus maximus muscles that were harvested following a single treadmill run (2.5 h, 10 m min^{-1}, 3% gradient) and compared to non-exercising controls ($n = 4$ mice per group). Mice were anaesthetized as described for Experiment 1; muscles were rapidly excised (bilaterally) and snap-frozen in liquid nitrogen. Glycogen measurements were normalized to total muscle protein (Bio-Rad, Hercules, CA, USA).

In the second protocol, mice ran on a treadmill once daily for 2 weeks. Training bouts lasted 30 min at 10 m min^{-1}, 3% gradient on the first day, increased to 1 h at 15 m min^{-1}, 8% gradient over the first week, and were held at 1 h, 16–17 m min^{-1} and 8% gradient for the second week. Control mice were housed in identical conditions adjacent to the training group ($n = 3$ mice per group). At the end of the 2-week training programme, trained and control mice were anaesthetized and perfused with fixative as described for Experiment 1. The left gluteus maximus muscle was then excised, embedded in paraffin, and 30 μm-thick cross-sections were obtained. Three sections located at least 100 μm apart from each other were taken from the mid region of each muscle

Table 1. Body mass and gluteus maximus muscle characteristics in Young, Adult and Old

	Young	Adult	Old
Body mass (g)	28 ± 0.2*	32 ± 0.4	33 ± 0.4
Muscle mass, wet (mg)	70 ± 4	69 ± 3	70 ± 5
Muscle mass, dry (mg)	17 ± 2	15 ± 1	15 ± 1
Muscle surface area (mm^2)	169 ± 5	176 ± 7	173 ± 4

*Body mass of Young ($n = 26$) was significantly lower than for Adult ($n = 17$) or Old ($n = 21$) ($P < 0.05$). Values for muscle mass and surface area ($n = 6$–10 per cell) were not significantly different across age-groups.

and processed for immunohistochemical labelling of the endothelial cell-specific marker CD31 (i.e. platelet endothelial cell adhesion molecule-1, PECAM-1; polyclonal rabbit antibody, 1 : 500; gift from Joseph Madri, Yale University) and subsequent fluorescence detection (Alexa Fluor 488 goat anti-rabbit lgG; Molecular Probes, Eugene, OR, USA). Three separate images of each section (~150 fibres per image) were acquired (Nikon E800, 10X objective; NA, 0.30) for a total of nine images per muscle. The capillary-to-fibre (C/F) ratio was determined by dividing the total number of capillaries by the total number of muscle fibres counted in the images from each muscle.

Statistical analyses. Data were analysed using one-way and repeated measures analysis of variance (Experiments 1–3) and unpaired *t* tests (recruitment studies) using Sigma Stat software (v.2.03 SPSS; Chicago, IL, USA). For Experiments 2 and 3, comparisons were made among age-groups within each stimulus level. When indicated, Tukey's *post hoc* comparisons were used to identify significantly different groups. For network architecture, $n = 5$ mice per age-group were used as described in Experiment 1. For *in vivo* experiments, *n* refers to the number of arterioles studied, with one 2A arteriole studied per mouse. Differences between groups were considered statistically significant when $P < 0.05$. Summary data are presented as mean values ± S.E.M.

Results

A total of 31 Young, 24 Adult and 28 Old were studied. Body mass was significantly greater in Adult and Old than in Young, attributable to the greater adiposity observed during dissections. Gluteus maximus muscle mass (wet and dry) and surface areas were not different across age-groups (Table 1).

Experiment 1: arteriolar network architecture

Arteriolar network analyses. The topology of the arteriolar network was well conserved within and across age-groups (Fig. 1). Arteriolar segment number (Fig. 2*A*), segment length (Fig. 3*A*), segment surface area (Fig. 3*B*), total segment length (Fig. 3*C*) and total segment surface area (Fig. 3*D*) were not different among age-groups. The number of arteriolar segments, their branch angles and their tortuosity all increased as vessel diameter decreased (Fig. 2). Although segment lengths (Fig. 3*A*) and surface areas (Fig. 3*B*) increased with vessel diameter, total segment lengths (Fig. 3*C*) and surface areas (Fig. 3*D*) were greatest for the smallest arterioles and least for the largest arterioles, reflecting corresponding differences in the number of segments (Fig. 2*A*). These topographical features are consistent with a network originating from a feed artery which branches into progressively smaller and more numerous segments (Fig. 1). For vessels 11–30 μm

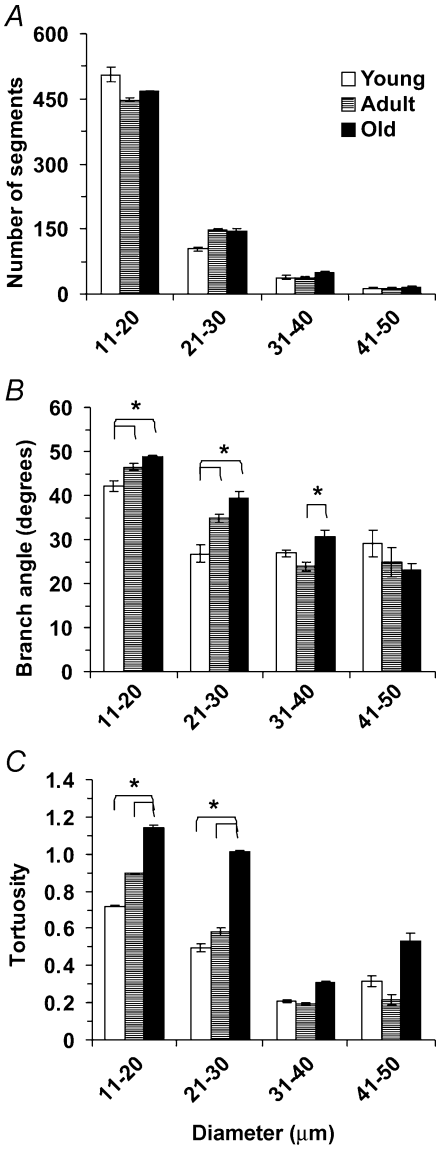

Figure 2. Number, branch angle and tortuosity of arteriolar segments computed from three-dimensional maps of the inferior gluteal artery network in the mouse gluteus maximus muscle
Values are given for arterioles in diameter bins of 10 μm (*x*-axes); $n = 5$ per age-group. *Pair-wise differences where $P < 0.05$.

in diameter, branch angles were greater in Old and Adult compared with Young (Fig. 2*B*; $P < 0.05$). These arterioles in Old were also more tortuous than corresponding segments from Adult or Young (Fig. 2*C*; $P < 0.05$).

Experiment 2: arteriolar tone, reactivity and conducted vasodilatation

Arteriolar reactivity to oxygen and agonists. Baseline and maximum diameters of 2A branches were not different across ages (Table 2) and the maximal diameters of these arterioles were not different from 2A branches studied with vascular casting (35–40 μm). With spontaneous resting tone, baseline diameters averaged 45% of maximum diameters. In response to elevating the oxygen level in the superfusion solution, vasoconstriction occurred in all age-groups but was ~2-fold greater in Young *versus* Adult or Old (Table 2, $P < 0.05$). When ACh or PE were added to the superfusion solution, there were no differences in response among age-groups (Fig. 4), nor was there a difference in maximum diameter between endothelium-dependent (ACh) and independent (SNP) vasodilatation.

Conducted vasodilatation. At the local site of ACh delivery, mean dilatations were 83, 90, 96 and 100% of maximum diameter (Table 2) for stimulus durations of 250, 500, 750 and 1000 ms, respectively. At both of the remote sites, the amplitude of conducted vasodilatation also increased with stimulus duration ($P < 0.05$; Fig. 5). At 500 μm upstream, conducted responses were not significantly different across age-groups for any stimulus duration. However, at 1000 μm, conducted vasodilatation (pooled across stimulus durations) was 7 ± 1 μm in Young, increased by ~2-fold in Adult (14 ± 2 μm), and was reduced markedly in Old (4 ± 1 μm; $P < 0.05$).

Experiment 3: arteriolar responses and active tension with muscle contraction

Arteriolar responses to muscle contraction. We tested whether vasodilatation during and following 30 s of muscle contraction was affected by age. A representative experimental record is shown in Fig. 6*A*. Across age-groups, functional dilatations increased with stimulation frequency ($P < 0.05$; Fig. 6) and were $48 \pm 4\%$, $60 \pm 3\%$ and $80 \pm 3\%$ of maximum diameters (see Table 2) at 2, 4 and 8 Hz, respectively. For all three stimulus frequencies, neither baseline diameters nor contraction-induced dilatations were different across age-groups, and arterioles consistently recovered to baseline diameter following contractions (Fig. 6*B*). Records representative of the mean responses during recovery from muscle contraction at 8 Hz are shown in Fig. 6*C*. At 4 and 8 Hz, vasodilatation returned to baseline faster in Old and Adult than in Young ($P < 0.05$; Fig. 6*D*). There was a significant main effect of age on the time required to recover from functional vasodilatation (Young > Adult > Old; $P < 0.05$).

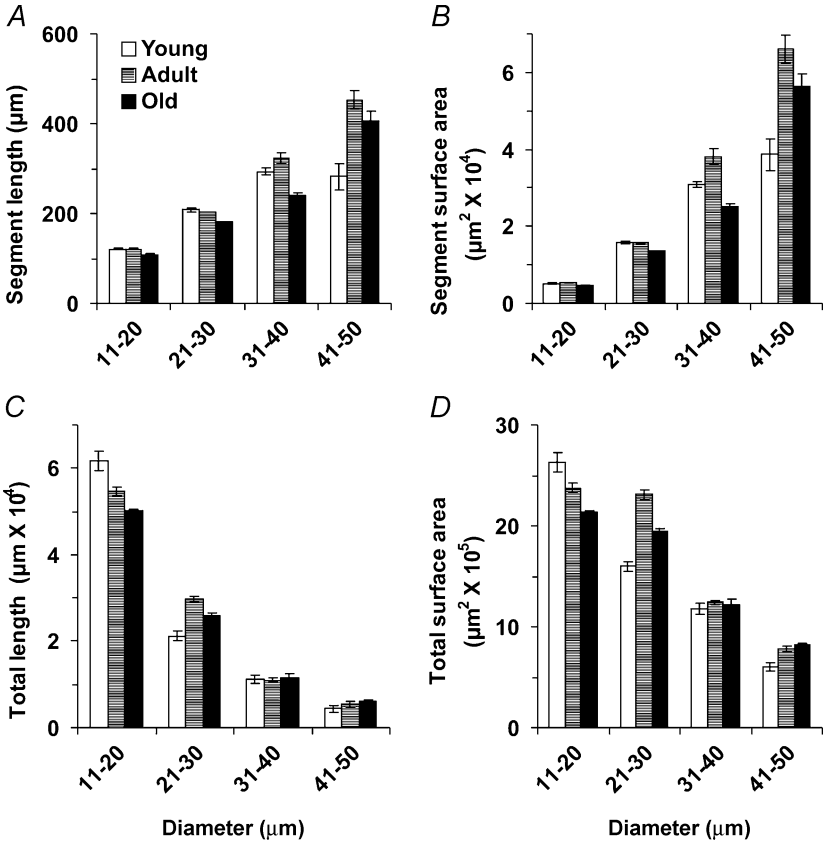

Figure 3. Arteriolar segment lengths and surface areas computed from three-dimensional maps of the inferior gluteal artery network in the mouse gluteus maximus muscle
Values are shown for individual segments (*A* and *B*) and for the sum (Total) of all segments (*C* and *D*) in diameter bins of 10 μm (*x*-axes); $n = 5$ per age-group. There were no significant differences across age-groups.

Table 2. Diameters of second-order arterioles in gluteus maximus muscles of Young, Adult and Old

Age-group	Baseline (μm)	Maximum (μm)	Oxygen (μm)
Young	18 ± 1	37 ± 1	-11 ± 1*
Adult	16 ± 1	37 ± 1	-5 ± 1
Old	16 ± 1	37 ± 1	-5 ± 1

Baseline values were recorded during spontaneous resting tone. Maximum values were recorded during exposure to SNP (10^{-5} M). Oxygen indicates the reduction in diameter from baseline during equilibration with 21% oxygen in the superfusion solution. There were no differences in baseline or maximum diameters between age-groups. *Arterioles in muscles of Young were more sensitive to oxygen than in Adult or Old, $P < 0.05$ ($n = 6$–10 per cell).

Active tension. Active tension produced during contractions of the gluteus maximus muscle was not different across age-groups or between 2, 4 and 8 Hz stimulation frequencies ($P > 0.05$); for all muscles pooled, the gluteus maximus muscle produced twitch tension (P_t) of 53 ± 3 mN mm^{-2} and maximal tetanic tension (P_o) of 148 ± 7 mN mm^{-2}. The twitch-to-tetanus ratio (P_t/P_o) was not different across stimulation frequencies among age-groups and averaged 0.36 ± 0.01 overall (Fig. 7*A*). The relationship between stimulation frequency and tension production was not different across age-groups (Fig. 7*B*) implying little or no change in fibre type in this muscle with ageing.

Muscle recruitment. Muscle glycogen content decreased from 1.8 ± 0.3 to 0.7 ± 0.1 mg (g protein)$^{-1}$ following a single exercise bout ($P < 0.05$), confirming that the gluteus maximus muscle is metabolically active during locomotion. Following a 2-week running programme, the C/F ratio increased from 1.41 ± 0.02 to 1.69 ± 0.06 ($P < 0.05$), confirming that the mouse gluteus maximus muscle responds to run-training with increased capillarity.

Discussion

This study is the first to investigate how ageing may affect the structure and function of arterioles controlling blood flow to a skeletal muscle of the mouse. As shown by glycogen depletion and capillary proliferation in response to treadmill running, the gluteus maximus muscle is active during locomotion. Based upon this model, our principle new findings are that arteriolar network architecture, endothelium-dependent vasodilatation and smooth muscle contraction to adrenoreceptor activation are highly conserved during ageing. In contrast, oxygen sensitivity was 2-fold greater in Young *versus* Adult or Old, conducted vasodilatation increased with maturation from Young to Adult and then decreased for Old, and the capacity to sustain postcontraction vasodilatation decreased progressively with age.

Arteriolar network architecture

There are few previous studies of age-related changes in vascular network architecture. In a longitudinal study of the mouse ear, the architecture of arteriolar networks remained nearly constant throughout ~20 months of life, though microvessels tended to elongate during the early postnatal months (Vollmar *et al.* 2000). In the cremaster muscle of Fischer-344 rats, random sampling of latex casts indicated that arteriolar segment lengths tended to increase with age (from 12 to 24 months) without changes in diameter (Cook *et al.* 1992). For arterioles of similar diameters, segment lengths reported here for the mouse gluteus maximus muscle (Fig. 3) are similar to those reported for the cremaster muscle of the rat (Cook *et al.* 1992) and hamster (Frame & Sarelius, 1993) as well as those in rat soleus and extensor digitorum longus muscles (Williams & Segal, 1992). This agreement across studies substantiates and validates the network analysis system developed here. The present data indicate that arteriolar network architecture in skeletal muscle is conserved throughout life in healthy, cage-sedentary mice (Figs 1–3). In addition to controlling blood flow, arterioles can provide a significant source of oxygen diffusion within skeletal muscle (Pittman, 2000). Thus, the present findings further indicate that the total surface area for the diffusion of oxygen from arterioles (Fig. 3*D*) remains stable with ageing.

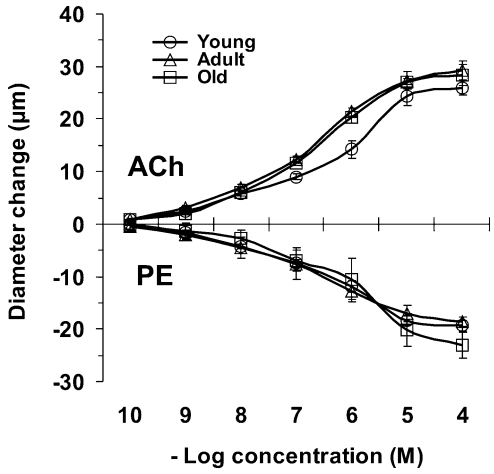

Figure 4. Vasodilatation and vasoconstriction in second-order arterioles of the mouse gluteus maximus muscle
Acetylcholine (ACh) or phenylephrine (PE) was added cumulatively to the superfusion solution (see Methods for details). There were no significant differences across age-groups; $n = 4$–5 per measurement.

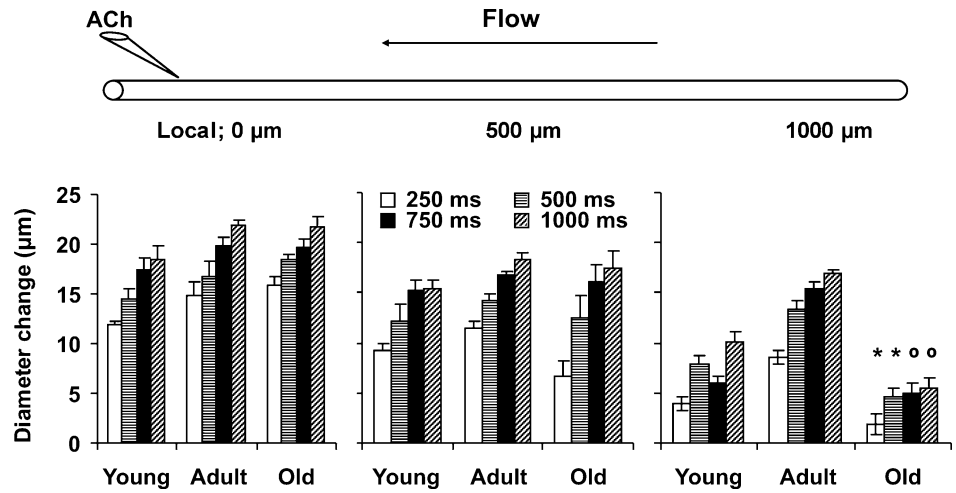

Figure 5. Local and conducted vasodilatation of arterioles in response to ACh
Diagram at top illustrates spatial relationships between ACh micropipette, arteriole under study and direction of blood flow. Vasodilator responses at local (0 μm) and conducted sites (500 and 1000 μm) are presented below respective positions in the diagram; $n = 6$–10 per age-group. Diameter changes are given for microiontophoresis pulse durations of 250, 500, 750 and 1000 ms (all at 1 μA). *Significantly different from other two age-groups (within pulse duration), $P < 0.05$; ^{o}significantly different *versus* Adult, $P < 0.05$.

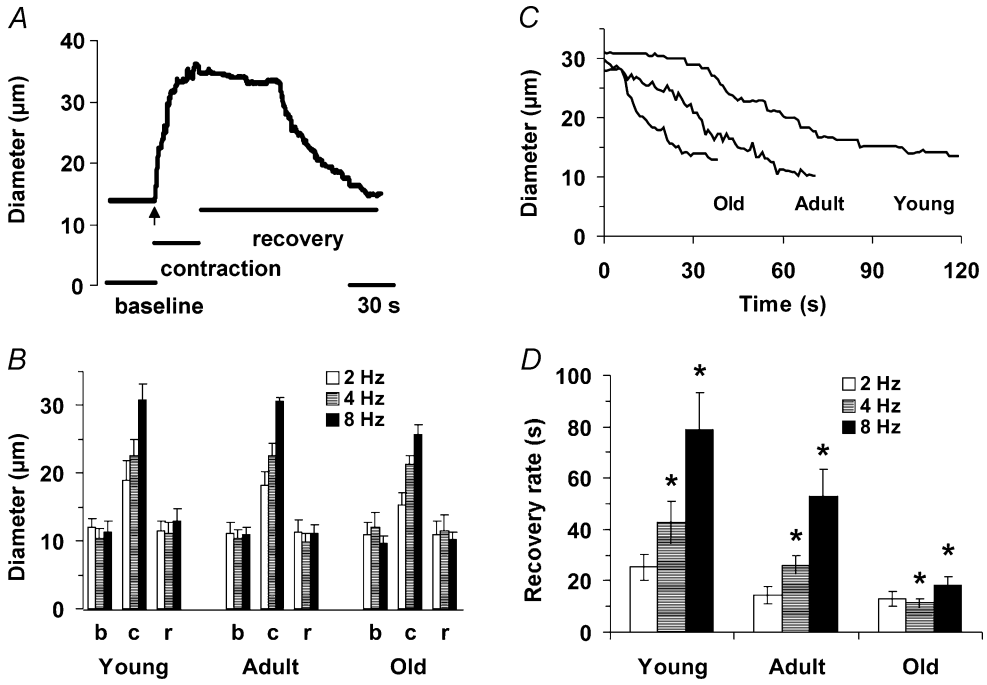

Figure 6. Arteriolar dilatation and recovery in response to muscle contraction
A, representative trace of 2A arteriole response to muscle contraction in Young (30 s at 8 Hz, onset of contractions at vertical arrow). *B*, b indicates the initial baseline diameter, c indicates peak diameter during muscle contraction, r indicates diameter at the end of recovery; b and r were not different. Contraction-induced dilatations increased with stimulation frequency ($P < 0.05$) but were not different across age-groups. *C*, representative traces from Young, Adult and Old illustrating the attenuation of postcontraction (8 Hz) vasodilatation with ageing; contractions ended at Time = 0. *D*, recovery rate indicates the respective times taken to return to within 37% of the original baseline diameter. *Significant difference across age-groups for all pair-wise comparisons within a given stimulation frequency; $P < 0.05$, $n = 6$–7 per age-group.

Topological analyses (Fig. 2) revealed increased branching angles and tortuosity in small arterioles of Old and Adult compared to Young. The values we obtained for tortuosity are consistent with those reported for venules in the mouse ear (Vollmar *et al.* 2000) as well as capillaries in skeletal muscle of dogs (Mathieu-Costello *et al.* 1989) and rats (Mathieu-Costello, 1987; Russell *et al.* 2003) of similar age-groups. In the mouse ear, venular tortuosity increased with ageing while that of arterioles did not (Vollmar *et al.* 2000). Increasing tortuosity is a common feature of ageing in larger arteries (Wenn & Newman, 1990). Age-related increases in tortuosity produce regions of low wall shear stress as do regions of turbulent flow generated by larger branch angles (Sidik & Mazumdar, 1994; Paszkowiak & Dardik, 2003). In conduit arteries, these haemodynamic conditions elevate the risk for intimal proliferation and atherosclerosis (Sidik & Mazumdar, 1994; Paszkowiak & Dardik, 2003). The functional consequences of such changes in much smaller arterioles remain to be determined.

Arteriolar reactivity to oxygen and agonists

With an increase in oxygen availability, the constriction of 2A branches in Young was 2-fold greater than in Adult or Old (Table 2). These findings are the first to suggest that there are age-related differences in the regulation of vasomotor tone in response to oxygen. Across age-groups, 2A branches responded similarly to ACh (vasodilatation) and PE (vasoconstriction) through their complete range of reactivity (Fig. 4). Further, our finding that maximum dilatations to ACh were not different from those to SNP indicates that the ability of the endothelium to drive smooth muscle cell relaxation is intact and similar regardless of age. Arterioles isolated from fast-twitch muscles (gastrocnemius) of young (4 months) and old (24 months) Fischer-344 rats have also shown no difference in dilatation in response to ACh (Muller-Delp *et al.* 2002*b*). However, arterioles isolated from slow-twitch muscles (soleus) of old rats showed significantly smaller dilatations in response to ACh when compared with young rats (Muller-Delp *et al.* 2002*b*). Consistent with the present findings using PE, constriction in response to noradrenaline (norepinephrine) was not affected by age in arterioles from either fast- or slow-twitch muscles (Muller-Delp *et al.* 2002*a*) suggesting that signalling events mediated through α-adrenoreceptor activation do not change appreciably with age. Nevertheless, the effects of ageing on microvascular reactivity may vary for different muscles.

Conducted vasodilatation

In response to ACh microiontophoresis, neither vasodilatation at the local site nor conducted responses at 500 μm upstream were different across age-groups. Thus, we propose that significant age-related differences in conduction at 1000 μm (Fig. 5) indicate complementary changes in cell-to-cell signalling (e.g. through gap junction channels) within the arteriolar wall that become manifest at greater distances from the site of initiation. The expression of connexin proteins, which comprise gap junction channels, decreases with ageing in rat aorta (Yeh *et al.* 2000) and in cultured endothelial cells (Xie & Hu, 1994). The decreases in conducted vasodilatation in Old that we observed may therefore reflect either altered expression of connexin proteins or impaired function of gap junction channels. Our finding that conducted vasodilatation was enhanced from Young to Adult (Fig. 5) suggests that cell-to-cell communication along the arteriolar wall is not fully developed in mice at 2–3 months of age. A question for future study is how maturation and ageing affect the expression and/or regulation of gap junctions in the microcirculation.

Arteriolar responses to muscle contraction

Force production was not different among age-groups across a 4-fold range of twitch frequencies (2, 4 and 8 Hz; Fig. 7*A*), suggesting that the same metabolic demand was produced consistently for each age-group. This conclusion

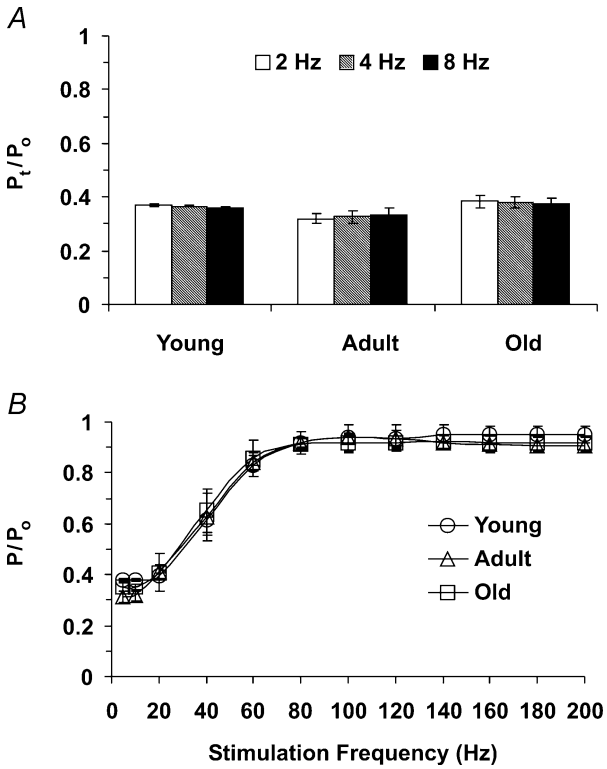

Figure 7. Active tension produced during muscle contractions
A, ratio of twitch tension (P_t) to peak tetanic tension (P_o) at 2, 4 and 8 Hz. There were no significant differences among age-groups ($n = 4$ each) or twitch frequencies. *B*, relationship between stimulation frequency and tension production (P) normalized to P_o, which was not different among age-groups (overall mean P_o, 148 ± 7 mN mm^{-2}).

is supported by our finding that vasodilatation at the end of contractions (Fig. 6*B*) and in response to topical administration of vasodilators (e.g. Fig. 4) was similar across age-groups. Moreover, arterioles from each group consistently recovered to their resting baseline following contractions at each level of activity. An unexpected finding was the difference in rates of recovery (Fig. 6*C* and *D*) across age-groups. The rapid return to baseline in Old relative to Young indicates an impairment in the ability to sustain vasodilatation, which may slow metabolite removal (Dodd *et al.* 1984). In turn, we suggest that the attenuation of postcontraction vasodilatation may delay recovery and reduce exercise tolerance when repeated bouts of activity are involved. For Young and Adult, there was a pattern of increasing time for recovery with increasing stimulation frequency (Fig. 6*D*). However, this pattern was not sustained in Old where stimulation at 2 and 4 Hz yielded similar recovery rates. Moreover, recovery from vasodilatation after 30 s of contractions was similar in the Adult 2 Hz as well as the Old 2 and 4 Hz conditions (∼17 s). This finding suggests that there may be a maximal rate for recovery following a given bout of muscle contractions that is intrinsic to the microvessels and insensitive to the frequency of muscle fibre contractions *per se*.

Muscle fibre type and function

The gluteus maximus is a muscle of mixed fibre type in rats and humans (Johnson *et al.* 1973; Armstrong & Phelps, 1984). Although fibre type has not been analysed for this muscle in the mouse, the ratio of twitch/tetanic tension (P_t/P_o) we obtained (0.36 ± 0.01; Fig. 7), is closer to that reported for fast-twitch extensor digitorum longus muscle (∼0.4) than for the slow-twitch soleus muscle (∼0.25) (Verburg *et al.* 2001). When taken with the reactivity we observed in response to ACh and PE discussed above, our *in vivo* data are therefore consistent with *in vitro* studies using arterioles taken from muscles of similar (mixed) fibre type (Muller-Delp *et al.* 2002*a*,*b*). Moreover, frequency–force plots (Fig. 7) were not different across age-groups, suggesting that fibre type in the gluteus maximus muscle was not appreciably affected by ageing (e.g. a transition to a slower fibre type would be expected to shift the frequency–force plot to the left).

Recruitment during locomotion

Development of the mouse gluteus maximus muscle for intravital microscopy presents new opportunities for the study of skeletal muscle microcirculation. In addition to the possibilities afforded by genetic manipulation in mice, this preparation has several benefits over previous models. For example, the gluteus maximus is common to both sexes, is found in all mammalian species, and is recruited during locomotion. Furthermore, a primary strength of this new preparation is the ability to evaluate intact vascular networks in their native muscle environment. Thus, the gluteus maximus muscle should prove useful as an experimental model in opening new avenues for the study of relationships between ageing, exercise and microvascular dysfunction.

Conclusion

The overall architecture of arteriolar networks in the mouse gluteus maximus muscle of mice was highly conserved across Young, Adult and Old, as were muscle mass and force production. There were no age-related differences in arteriolar segment numbers, lengths or surface areas although tortuosity and branching angle of the smallest arterioles increased with age. While the vasoconstrictor response to elevated oxygen levels was greatest in Young, the local vasomotor responses to endothelium-dependent (ACh) and independent (SNP) vasodilators were maintained across age-groups, as was vasoconstriction following administration of PE. The ability to conduct vasodilatation along the arteriolar wall increased from Young to Adult and then declined in Old, suggesting that the efficacy of cell-to-cell signalling along the arteriolar wall increases and then decreases over the life span. Further, the ability to sustain vasodilatation following muscle contraction was impaired in Old, which may compromise recovery and tolerance to intermittent physical activity. The present findings illustrate a dynamic interaction between age and arteriolar function in skeletal muscle that may play a key role in affecting exercise tolerance independent of changes in muscle mass or contractile properties.

References

Armstrong RB & Phelps RO (1984). Muscle fiber type composition of the rat hindlimb. *Am J Anat* **171**, 259–272.

Cohen KD & Sarelius IH (2002). Muscle contraction under capillaries in hamster muscle induces arteriolar dilatation via K (ATP) channels and nitric oxide. *J Physiol* **539**, 547–555.

Cook JJ, Wailgum TD, Vasthare US, Mayrovitz HN & Tuma RF (1992). Age-related alterations in the arterial microvasculature of skeletal muscle. *J Gerontol* **47**, B83–B88.

Dodd S, Powers SK, Callender T & Brooks E (1984). Blood lactate disappearance at various intensities of recovery exercise. *J Appl Physiol* **57**, 1462–1465.

Dutta C, Hadley EC & Lexell J (1997). Sarcopenia and physical performance in old age: overview. *Muscle Nerve* **5**, (Suppl.) S5–S9.

Figueroa XF, Paul DL, Simon AM, Goodenough DA, Day KH, Damon DN & Duling BR (2003). Central role of connexin40 in the propagation of electrically activated vasodilation in mouse cremasteric arterioles in vivo. *Circ Res* **92**, 793–800.

Frame MD & Sarelius IH (1993). Arteriolar bifurcation angles vary with position and when flow is changed. *Microvasc Res* **46**, 190–205.

Hungerford JE, Sessa WC & Segal SS (2000). Vasomotor control in arterioles of the mouse cremaster muscle. *FASEB J* **14**, 197–207.

Irion GL & Vasthare US &Tuma RF (1987). Age-related change in skeletal muscle blood flow in the rat. *J Gerontol* **42**, 660–665.

Johnson MA, Polgar J, Weightman D & Appleton D (1973). Data on the distribution of fibre types in thirty-six human muscles. An autopsy study. *J Neurol Sci* **18**, 111–129.

Lawrenson L, Poole JG, Kim J, Brown C, Patel P & Richardson RS (2003). Vascular and metabolic response to isolated small muscle mass exercise: effect of age. *Am J Physiol Heart Circ Physiol* **285**, H1023–H1031.

Lexell J (1995). Human aging, muscle mass, and fiber type composition. *J Gerontol A Biol Sci Med Sci* **50**, 11–16.

Mathieu-Costello O (1987). Capillary tortuosity and degree of contraction or extension of skeletal muscles. *Microvasc Res* **33**, 98–117.

Mathieu-Costello O, Hoppeler H & Weibel ER (1989). Capillary tortuosity in skeletal muscles of mammals depends on muscle contraction. *J Appl Physiol* **66**, 1436–1442.

Muller-Delp JM, Spier SA, Ramsey MW & Delp MD (2002*b*). Aging impairs endothelium-dependent vasodilation in rat skeletal muscle arterioles. *Am J Physiol Heart Circ Physiol* **283**, H1662–H1672.

Muller-Delp JM, Spier SA, Ramsey MW, Lesniewski LA, Papadopoulos A, Humphrey JD & Delp MD (2002*a*). Effects of aging on vasoconstrictor and mechanical properties of rat skeletal muscle arterioles. *Am J Physiol Heart Circ Physiol* **282**, H1843–H1854.

Paszkowiak JJ & Dardik A (2003). Arterial wall shear stress: observations from the bench to the bedside. *Vasc Endovascular Surg* **37**, 47–57.

Pittman RN (2000). Oxygen supply to contracting skeletal muscle at the microcirculatory level: diffusion vs. convection. *Acta Physiol Scand* **168**, 593–602.

Proctor DN, Shen PH, Dietz NM, Eickhoff TJ, Lawler LA, Ebersold EJ, Loeffler DL & Joyner MJ (1998). Reduced leg blood flow during dynamic exercise in older endurance-trained men. *J Appl Physiol* **85**, 68–75.

Russell JA, Kindig CA, Behnke BJ, Poole DC & Musch TI (2003). Effects of aging on capillary geometry and hemodynamics in rat spinotrapezius muscle. *Am J Physiol Heart Circ Physiol* **285**, H251–H258.

Segal SS (1991). Microvascular recruitment in hamster striated muscle: role for conducted vasodilation. *Am J Physiol* **261**, H181–H189.

Segal SS & Duling BR (1989). Conduction of vasomotor responses in arterioles: a role for cell-to-cell coupling? *Am J Physiol* **256**, H838–H845.

Sidik WA & Mazumdar JN (1994). A mathematical study of turbulent blood flow through an arterial bifurcation. *Australas Phys Eng Sci Med* **17**, 1–13.

Verburg E, Thorud HM, Eriksen M, Vollestad NK & Sejersted OM (2001). Muscle contractile properties during intermittent nontetanic stimulation in rat skeletal muscle. *Am J Physiol Regul Integr Comp Physiol* **281**, R1952–R1965.

Vollmar B, Morgenthaler M, Amon M & Menger MD (2000). Skin microvascular adaptations during maturation and aging of hairless mice. *Am J Physiol Heart Circ Physiol* **279**, H1591–H1599.

Wahren J, Saltin B, Jorfeldt L & Pernow B (1974). Influence of age on the local circulatory adaptation to leg exercise. *Scand J Clin Lab Invest* **33**, 79–86.

Wenn CM & Newman DL (1990). Arterial tortuosity. *Australas Phys Eng Sci Med* **13**, 67–70.

Williams DA & Segal SS (1992). Microvascular architecture in rat soleus and extensor digitorum longus muscles. *Microvasc Res* **43**, 192–204.

Xie HQ & Hu VW (1994). Modulation of gap junctions in senescent endothelial cells. *Exp Cell Res* **214**, 172–176.

Yeh HI, Chang HM, Lu WW, Lee YN, Ko YS, Severs NJ & Tsai CH (2000). Age-related alteration of gap junction distribution and connexin expression in rat aortic endothelium. *J Histochem Cytochem* **48**, 1377–1389.

Acknowledgements

This work was supported by the United States Public Health Service, NIH grants R21-AG19347 and R01-HL41026. S.E.B. was supported by NIH T32-NS07455.

Authors' present addresses

S. E. Bearden: Department of Biological Sciences, Idaho State University, Pocatello, ID 83209, USA.

G. W. Payne: Faculty of Medicine, University of Northern British Columbia, Prince George, BC, Canada V2N 4Z9.